Tin Perovskite / Fullerene Planar Layer Photovoltaics: Improving the Efficiency and Stability of Lead-Free Devices

Kenneth P. Marshall[a], Richard I. Walton[a] and Ross A. Hatton[a*]

Department of Chemistry, University of Warwick, CV4 7AL, United Kingdom.

Supporting Information

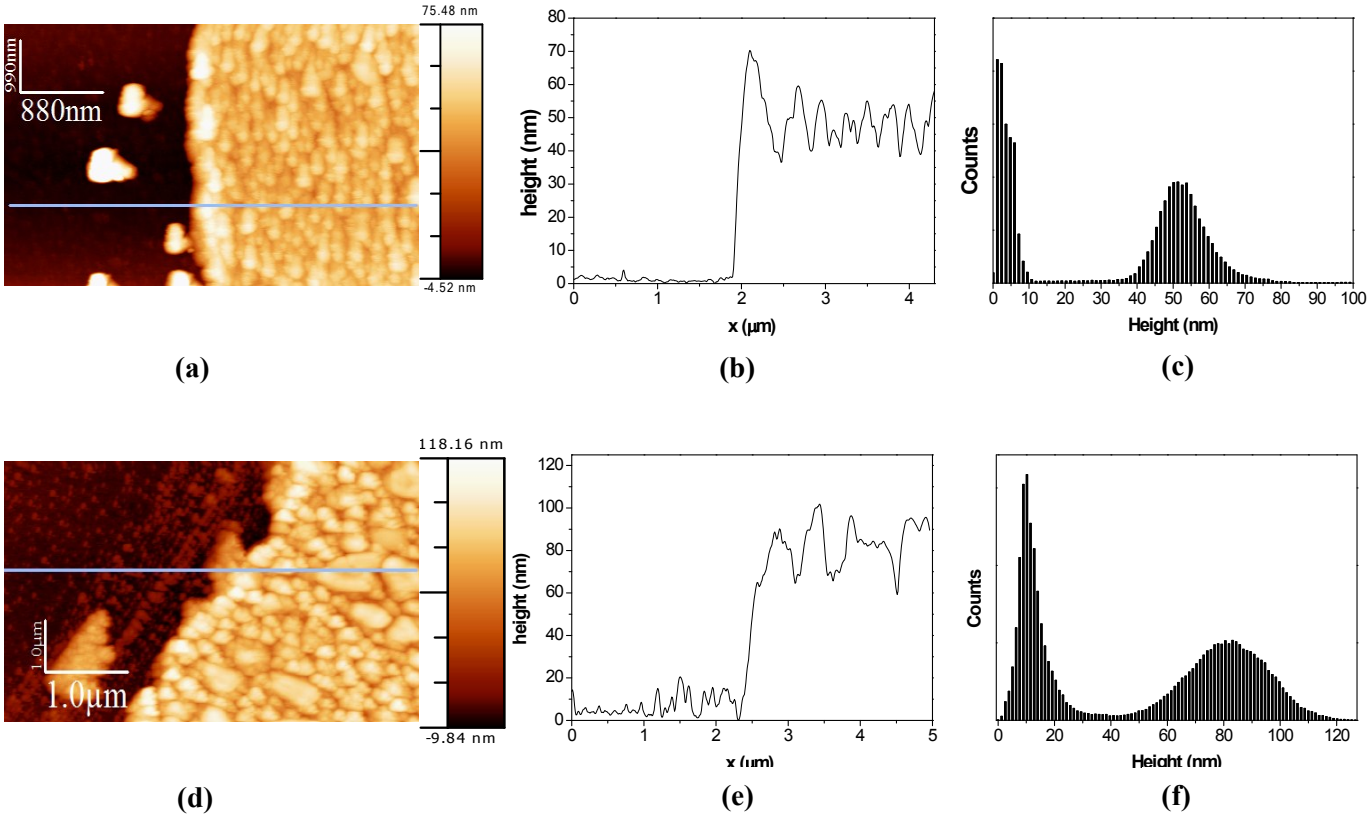

Figure S1: (a) An AFM image of a step edge in a scored $CsSnI_3$ film on glass prepared with 10% excess SnI_2. The film was spun cast at 4000 rpm from an 8 wt.% DMF solution. The apparent downward alignment of crystallites in image (a) is an image artefact.; **(b)** A representative cross-section of the AFM image shown in (a). This film is 40 – 60 nm in thickness and has a mean thickness of 50 nm, from the histogram shown in (c).; (d), (e), and (f) show an AFM image, a representative cross-section of the AFM image, and a histogram of the step edge shown for a 15 wt.% $CsSnI_3$ film spin cast at 4000 rpm onto glass respectively. This film has a height of 50 – 90 nm with an average height of ~73 nm.

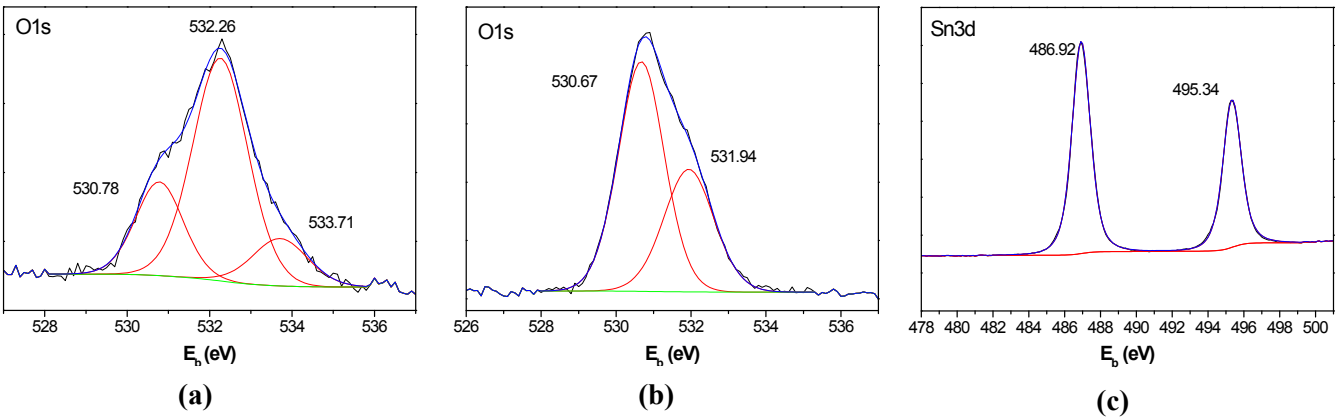

Figure S2: High resolution XPS spectra and peak fitting for: **(a)** O1s of $CsSnI_3$ film prepared from stoichiometric quantities of CsI and SnI_2.; **(b)** O1s region for $CsSnI_3$ oxidised in air for 5 hours. The peaks at ~530.7 eV and ~531.9 eV are indicative of SnO_2[1,2] and adsorbed O_2[3] respectively.; **(c)** Sn 3d region for $CsSnI_3$ oxidised for 5 hours. There are two peaks due to spin-orbit splitting that correspond to electrons from the $3d_{5/2}$ and $3d_{3/2}$ states. The difference in binding energy of Sn 3d electrons in Cs_2SnI_6 and SnO_2[2,4] cannot be resolved.

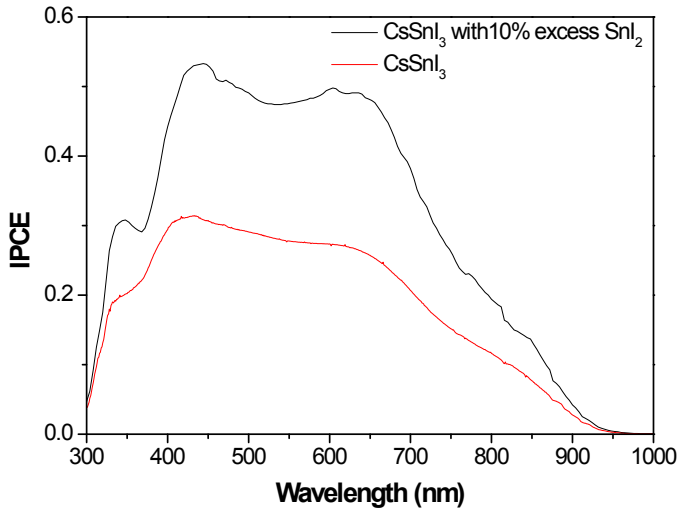

Figure S3: IPCE of ITO | CuI | $CsSnI_3$ | C_{60} (black - 10% excess SnI_2) or $PC_{60}BM$ (red - 0% excess SnI_2) | BCP | Al device.

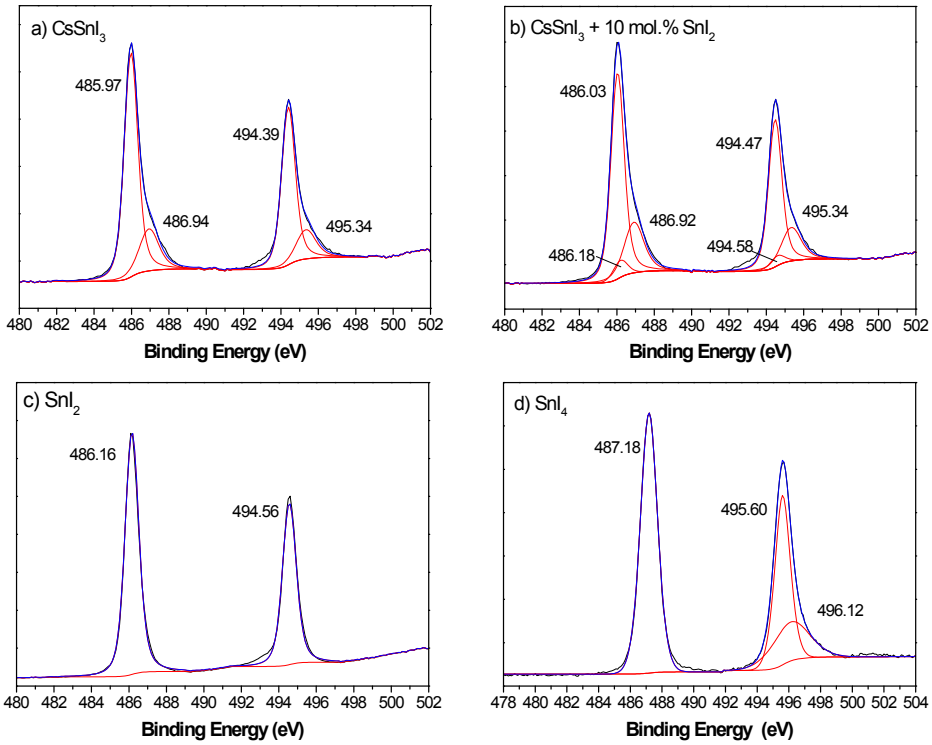

Figure S4: High resolution XPS spectra and peak fitting of the Sn 3d region for: **(a)** a $CsSnI_3$ film prepared from stoichiometric quantities of CsI and SnI_2. The shoulder at high binding energy on both peaks is assigned to Sn in a Cs_2SnI_6 environment. The binding energies for Sn in a Cs_2SnI_6 environment are given in Figure S2 (c). Cs_2SnI_6 is present because the sample is unavoidably exposed to air for ~ 1 minute when being transferred from the nitrogen filled glove box to the spectrometer vacuum system; **(b)** a $CsSnI_3$ film prepared with 10 mol % excess SnI_2. Notably, the peak fitting includes a small peak that can be assigned to Sn in a SnI_2 environment. The XPS spectrum for Sn 3d electrons in SnI_2 is given in **(c)**. Since ~ 95% of the photoelectrons originate from the top ~ 7 nm of the sample surface such a small SnI_2 peak is consistent with a very small amount of SnI_2 at the $CsSnI_3$ surface; **(c)** a SnI_2 film prepared by thermal evaporation; **(d)** a SnI_4 film prepared by thermal evaporation.

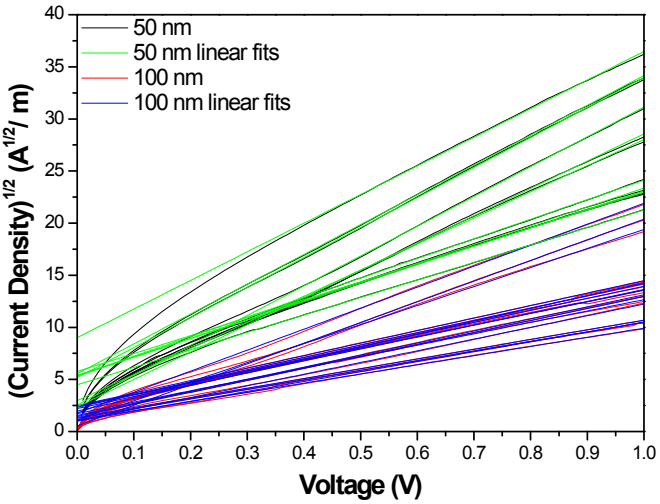

Figure S5: $J^{0.5}$ *vs.* V graph for unipolar diodes with structure: ITO glass | MoO_3 | SnI_2 (50 or 100 nm)| MoO_3| Al. The hole mobility is extracted from the gradient assuming a trap free space charge limited current and $\varepsilon_r = 30.30$.[5]

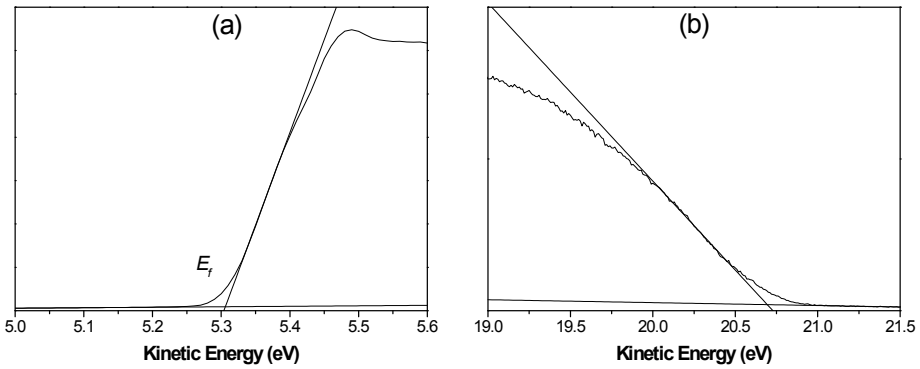

Figure S6: UPS spectra showing the secondary electron cut-off **(a)** and valence band edge **(b)** regions for CuI from which the ionization potential is estimated to be 5.84 eV ± 0.05 eV. Measurements were performed on 50 nm CuI films thermally evaporated onto Au substrates.

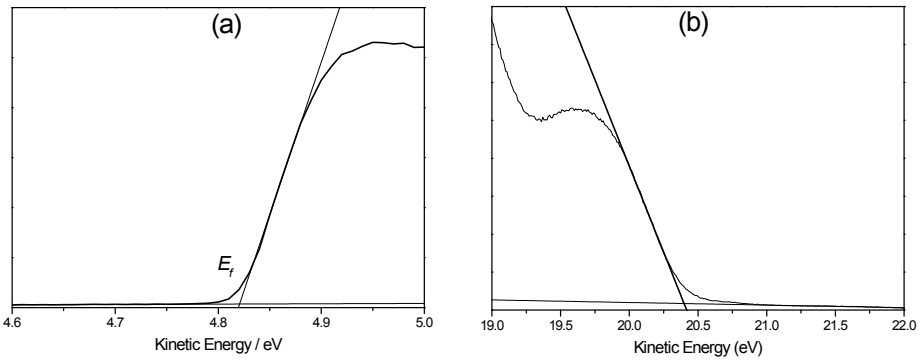

Figure S7: UPS spectra showing the secondary electron cut-off **(a)** and valence band edge **(b)** regions for SnI_2 on Au. The film was evaporated at 0.5 – 1 Å s^{-1} to a thickness of 30 nm.

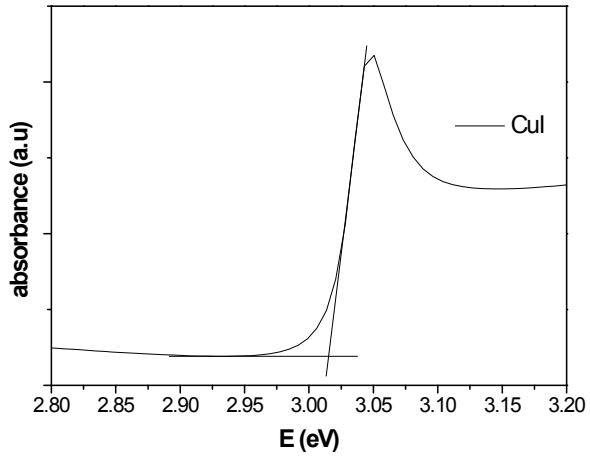

Figure S8: UV/ Vis/ NIR absorbance spectrum of a 100 nm CuI film deposited on glass by thermal evaporation. The E_g is estimated to be ~ 3.02 eV.

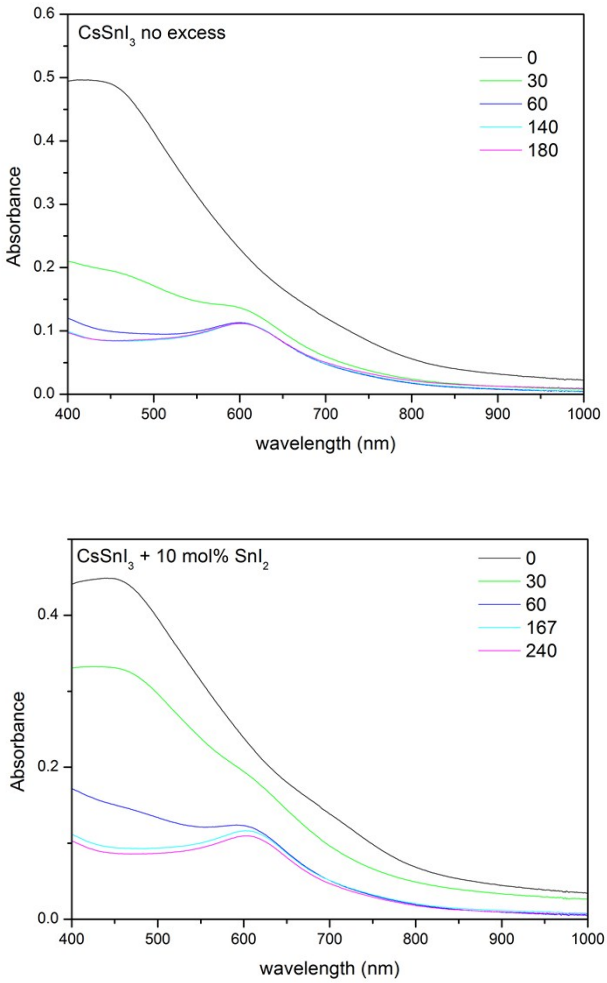

Figure S9: Absorption spectrum of $CsSnI_3$ films spun cast at 4000 rpm from an 8 wt.% DMF solution onto glass with 0 mol% (top) and 10 mol% (bottom) excess SnI_2, measured at various time intervals (in minutes) after exposure to laboratory air. The spectra convert from that of $CsSnI_3$ to that of Cs_2SnI_6 over a time frame of ~ 60 minutes. However, perovskite films sandwiched between the charge transport layers and electrodes in a PV device are expected to oxidise more slowly than a perovskite film on glass (as above) and so the rate of oxidation of the isolated film cannot be compared directly with the rate of device degradation.

Device	n	V_{oc} / V	J_{sc} / mA cm^{-2}	FF	η / %	η (best) / %
C_{60} (40nm), using solution processable CuI	18	0.243 ± 0.024	11.43 ± 0.89	0.413 ± 0.028	1.16 ± 0.21	1.40
C_{60} (40 nm) no CuI	17	0.262 ± 0.031	11.67 ± 0.50	0.375 ± 0.022	1.16 ± 0.18	1.40
C_{60} (40nm) 100 nm CuI	18	0.282 ± 0.030	11.6 ± 1.0	0.434 ± 0.032	1.42 ± 0.23	1.72
$PC_{61}BM$ (15mg ml^{-1}) no CuI	11	0.261 ± 0.042	8.6 ± 1.1	0.42 ± 0.065	1.02 ± 0.39	1.59
PCBM (15 mg ml^{-1}), 70 nm CuI	16	0.355 ± 0.026	8.94 ± 0.27	0.538 ± 0.043	1.72 ± 0.26	2.07
ICBA (7mg ml^{-1}, 1000 rpm) no CuI	17	0.352 ± 0.033	10.7 ± 1.8	0.468 ± 0.075	1.79 ± 0.56	2.65
ICBA (5 mg ml^{-1}) 100 nm CuI	16	0.491 ± 0.057	7.01 ± 0.68	0.500 ± 0.045	1.73 ± 0.44	2.60
ICBA (3 mg ml^{-1}) 100 nm CuI	14	0.430 ± 0.061	12.30 ± 0.48	0.395 ± 0.053	2.13 ± 0.53	2.76

Table S1: Key PPV device characteristics summarizing the performance of devices using 10 mol% excess SnI_2 in the $CsSnI_3$ layer and different electron acceptors with and without a CuI HTL. Also included in the table is data relating to devices fabricated using a solution processed CuI layer. The errors are given as ± 1 S.D. n is the device sample size in each case.

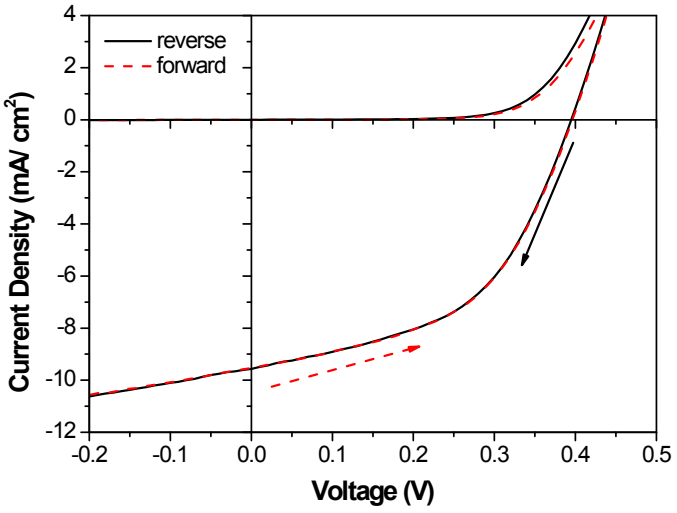

Figure S10: JV curve of individual ITO| CuI| $CsSnI_3$| $PC_{61}BM$| BCP| Al device with forward (−1 V to +1 V) and reverse (+1 V to −1 V) scans showing negligible hysteresis effect.

References

1. P. R. Moses, L. M. Wier, J. C. Lennox, H. O. Finklea, J. R. Lenhard, and R. W. Murray, *Anal. Chem.*, 1978, **50**, 576–585.
2. W.-K. Choi, H.-J. Jung, and S.-K. Koh, *J. Vac. Sci. Technol. A Vacuum, Surfaces, Film.*, 1996, **14**, 359–366.
3. A. Pashutski, A. Hoffman, and M. Folman, *Surf. Sci. Lett.*, 1989, **208**, L91–L97.
4. S. Suzer, T. Voscoboinikov, K. R. Hallam, and G. C. Allen, *Fresenius. J. Anal. Chem.*, 1996, **355**, 654–656.
5. C. C. Desai, J. L. Rai, and A. D. Vyas, *J. Mater. Sci.*, 1982, **17**, 3249–3252.